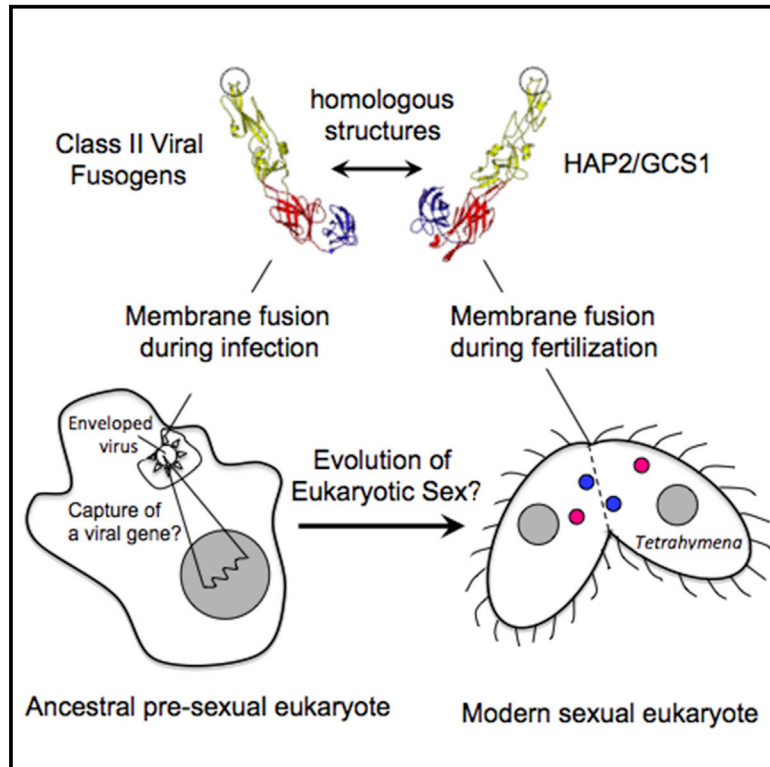


Current Biology

Structure-Function Studies Link Class II Viral Fusogens with the Ancestral Gamete Fusion Protein HAP2

Graphical Abstract



Authors

Jennifer Fricke Pinello, Alex L. Lai, Jean K. Millet, Donna Cassidy-Hanley, Jack H. Freed, Theodore G. Clark

Correspondence

tgc3@cornell.edu

In Brief

HAP2/GCS1 is deeply rooted in evolution and required for gamete fusion in diverse species. Pinello et al. demonstrate that a HAP2 ortholog from *Tetrahymena* closely resembles class II viral fusogens. From an evolutionary standpoint, it is unclear which came first, but HAP2's emergence may have been a critical step in the evolution of eukaryotic sex.

Highlights

- HAP2/GCS1 and class II viral fusogens adopt a remarkably similar protein fold
- HAP2 mediates membrane pore formation in mating *Tetrahymena* cells
- The *T. thermophila* HAP2 ortholog has a functional fusion loop peptide
- HAP2 may have arisen from a virus and been key to the origin of eukaryotic sex



Structure-Function Studies Link Class II Viral Fusogens with the Ancestral Gamete Fusion Protein HAP2

Jennifer Fricke Pinello,¹ Alex L. Lai,² Jean K. Millet,¹ Donna Cassidy-Hanley,¹ Jack H. Freed,² and Theodore G. Clark^{1,3,*}

¹Department of Microbiology and Immunology, Cornell University, Ithaca, NY 14853, USA

²Department of Chemistry and Chemical Biology, Cornell University, Ithaca, NY 14853, USA

³Lead Contact

*Correspondence: tgc3@cornell.edu

<http://dx.doi.org/10.1016/j.cub.2017.01.049>

SUMMARY

The conserved transmembrane protein, HAP2/GCS1, has been linked to fertility in a wide range of taxa and is hypothesized to be an ancient gamete fusogen. Using template-based structural homology modeling, we now show that the ectodomain of HAP2 orthologs from *Tetrahymena thermophila* and other species adopt a protein fold remarkably similar to the dengue virus E glycoprotein and related class II viral fusogens. To test the functional significance of this predicted structure, we developed a flow-cytometry-based assay that measures cytosolic exchange across the conjugation junction to rapidly probe the effects of HAP2 mutations in the *Tetrahymena* system. Using this assay, alterations to a region in and around a predicted “fusion loop” in *T. thermophila* HAP2 were found to abrogate membrane pore formation in mating cells. Consistent with this, a synthetic peptide corresponding to the HAP2 fusion loop was found to interact directly with model membranes in a variety of biophysical assays. These results raise interesting questions regarding the evolutionary relationships of class II membrane fusogens and harken back to a long-held argument that eukaryotic sex arose as the byproduct of selection for the horizontal transfer of a “selfish” genetic element from cell to cell via membrane fusion.

INTRODUCTION

Although sperm-egg fusion is a critical step in sexual reproduction, remarkably little is known about the molecular details of the process. Nevertheless, discovery of the conserved transmembrane protein, HAP2/GCS1 [1, 2], has brought renewed focus to the problem and raised the intriguing possibility that HAP2 is an ancestral gamete fusogen dating to the last common ancestor of all eukaryotes [3].

Based on gene deletion studies, HAP2 is required for fertilization in a wide range of taxa, although its activity appears restricted to sperm (or the functional equivalent of male gametes)

in sexually dichotomous species [1, 2, 4–7]. The model ciliate, *Tetrahymena thermophila*, on the other hand, expresses HAP2 in all seven of its mating types, and a complete block to fertility occurs only when the corresponding gene is deleted from both cells of a mating pair [7]. Other studies localizing HAP2 to regions of the plasma membrane where gamete fusion is initiated have suggested a direct role in membrane fusion [4, 7]; nevertheless, primary sequence comparisons between HAP2 homologs and known membrane fusogens have shown no obvious similarities [3]. Indeed, our current understanding of HAP2 structure-function relationships is based almost entirely on the effects of targeted mutations to the extracellular and cytosolic regions of the protein on fertilization success. In short, these studies suggest that species-restricted functions of HAP2 reside within the extracellular region, with numerous residues/motifs, including the conserved HAP2-GCS1 domain, having a role in HAP2 function [8, 9]. By contrast, some studies suggest that the cytosolic region is almost entirely dispensable for activity [8], whereas others point to positively charged residues as well as multi-cysteine motifs that may be palmitoylated as being important [9, 10].

Whereas the use of engineered mutations has been informative, assays for HAP2 function have focused largely on blocks to fertility rather than membrane fusion per se. Such assays are indirect and often time consuming, as are more direct assays for membrane fusion involving transmission electron microscopy. To address these issues in *Tetrahymena*, we sought to develop a quantitative flow-cytometry-based assay that would use exchange of fluorescently labeled proteins across the conjugation junction as a rapid and direct way to measure membrane pore formation in populations of synchronously mating cells. Concomitantly, we used template-based structural homology modeling to uncover conformational domains within HAP2 that are important for protein function. As shown here, predicted structures for the *T. thermophila* HAP2 ectodomain bear a striking resemblance to class II viral fusogens, such as the dengue virus E glycoprotein, and include a predicted fusion loop, which plays a key role in the infectious entry pathway of many viruses. Deletion of the predicted HAP2 fusion loop or residues thought to stabilize the loop were found to block pore formation in mating *Tetrahymena*, and a synthetic peptide corresponding to this region was found to interact directly with model membranes in a variety of biophysical assays. During the course of this work, we became aware of successful efforts to crystallize and

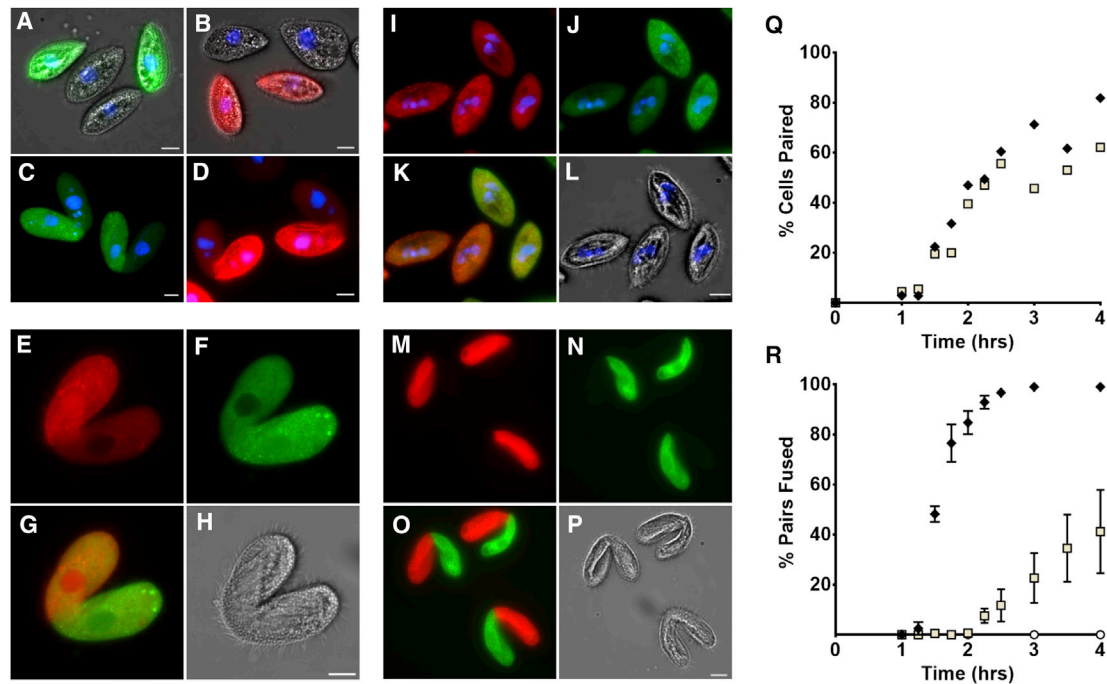


Figure 1. Conjugation Leads to Rapid Exchange of Labeled Cytosolic Proteins in Mating *T. thermophila*

Cells of different mating types were labeled with either carboxyfluorescein diacetate succinimidyl ester (CFSE) or Cell Trace Far Red (CTFR) and examined microscopically after fixation. Scale bars in all micrographs represent 10 μ m.

(A and B) Overlay of phase and fluorescence images of labeled and unlabeled cells combined and fixed 15 min post-mixing showing either green (A) or red (B) labeling (but no exchange of fluorescent proteins).

(C and D) Fluorescence images of labeled and unlabeled partners combined and fixed at 3.5 (C) and 2.5 hr (D) post-mixing, respectively. Partial exchange of fluorescent proteins from labeled (bright) to unlabeled (faint) mating partners is seen.

(E and F) Fluorescence image of a wild-type pair of cells in which both mating partners were separately labeled, combined, and fixed 3.5 hr post-mixing. Reciprocal exchange of labeled proteins is visible in the same mating pair viewed with either red (E) or green (F) filter sets.

(G) Merged image of (E) and (F).

(H) Phase image of the mating pair in (E)–(G).

(I and J) Fluorescence images of wild-type cells with one mating partner labeled with CTFR and the other with CFSE, imaged at 20 hr after mixing with red (I) or green (J) filter sets. At this time point, pairs have come apart, but exconjugant progeny cells maintain a combination of the parental fluorescent markers.

(K) Merged image of (I) and (J).

(L) Phase image of the cells in (I)–(K).

(M–P) A cross between Δ HAP2 partners of different mating types that were initially labeled with either CTFR or CFSE and visualized with red (M) and green (N) filter sets at 3.5 hr after mating as in (E)–(H). Note the absence of fluorescent protein transfer.

(Q) Representative data from one experiment showing the kinetics of pairing for WT \times WT (\blacklozenge) and WT \times Δ HAP2 (\square) crosses.

(R) The kinetics of fusion in WT \times WT (\blacklozenge), WT \times Δ HAP2 (\square), and Δ HAP2 \times Δ HAP2 (\circ) crosses determined as the percentage of pairs showing visible transfer of fluorescent material at the indicated time points. Data are expressed as the mean \pm SEM for three and four independent experiments (\blacklozenge and \square , respectively) and for one experiment (\circ).

generate a high-resolution structure for *Chlamydomonas* HAP2, along with functional data that are consistent with the results reported here [11]. Together, these studies argue strongly that HAP2 mediates fertilization through a membrane-fusion mechanism analogous to that used by dengue and related viruses to enter host cells.

RESULTS

Transfer of Labeled Cytosolic Proteins between Mating Cells

In *T. thermophila*, HAP2 is localized to the conjugation junction, a specialized region of membrane between the two mating cells where hundreds of fusion pores form [7, 12]. These pores allow the exchange of haploid pronuclei as well as limited amounts

of protein and RNA between mating partners. To determine whether the exchange of cytosolic material during sexual conjugation could be used to assay for membrane pore formation (referred to hereafter as membrane-fusion events), live cells of different mating types were starved to render them mating competent and their proteins labeled separately either green or red with the amine-reactive dyes, carboxyfluorescein diacetate succinimidyl ester (CFSE), or cell trace far-red (CTFR) [13]. Cells were then washed and mated with either unlabeled cells of a different mating type or with each other. In the case of wild-type (WT) cells, no exchange of labeled protein was visible by fluorescence microscopy prior to pairing (Figures 1A and 1B). After pairing, however, content exchange was readily detected between labeled and unlabeled cells (Figures 1C and 1D), as was the reciprocal exchange of fluorescent protein between

cells that were initially labeled either green or red (Figures 1E–1H). When these paired cells separated after the completion of mating (12–16 hr post-mixing), the vast majority had both fluorescent markers but were more intensely labeled one color or the other (Figures 1I–1L). Finally, no exchange of labeled protein was seen when mating types lacking the *HAP2* gene ($\Delta HAP2$ strains) were crossed (Figures 1M–1P), a result that was entirely expected because these cells are unable to form junctional pores [7].

By observing cells at varying time points after mixing, it was possible to determine the relative kinetics of membrane-fusion events with respect to pairing in this system. As shown in Figure 1Q, measurable numbers of pairs began to form 1 hr 15 min after mixing labeled WT cells of different mating types (30°C). By 1 hr 30 min, 50% of all WT pairs had exchanged dye, indicating that fusion pores form rapidly following the adhesion of mating cells (Figure 1R). Notably, the rate at which cells form pores (but not the rate of pairing) was significantly reduced when $\Delta HAP2$ strains were mated with a WT partner (Figures 1Q and 1R).

Quantitation of Membrane Fusion Using Flow Cytometry

The ability to detect exchange of fluorescent proteins across the conjugation junction enabled the use of flow cytometry to quantify the percentage of cells undergoing membrane fusion events in large-scale mating cultures. When cultures of WT cells (Figure 2A) containing two different mating types were labeled, mixed, and acquired by flow cytometry prior to pairing, two fluorescently labeled populations were seen: one CFSE^{hi} and the other CTFR^{hi} (Figure 2B). However, when the same cultures were fixed after the cells had completed mating and come apart, an entirely different pattern was observed (Figure 2C). In this case, the vast majority of cells (typically ~80%) contained both fluorescent tracers and fell into two equally sized populations: one brighter for CFSE and the other brighter for CTFR (“mid” fluorescence gate in Figure 2C). These cells had clearly undergone membrane fusion and exchanged labeled protein during the mating process. In addition to these mid-fluorescence events, three other populations were visible. The smallest (typically <10% of cells) was intensely labeled with both tracers (CFSE^{hi}/CTFR^{hi}; Figures 2C–2E, upper right-hand “pairs” gate) and most likely represented either persistent pairs (i.e., cells that had paired and failed to come apart) or pairs that formed very late in mating cultures. Indeed, a few pairs were visible by microscopy even 16 hr post-mixing, and based on forward light scattering (FSC), the size distribution of individual events in the pairs gate was consistently larger than that in the other gates (Figure 2F). The remaining two populations (comprising 10%–15% of total cells) were single labeled and expressed either CFSE^{hi} or CTFR^{hi} (Figure 2C). Cells in these populations had not acquired label from a mating partner and were the expected number of cells that fail to generate true (that is, cross-fertilized) progeny in standard WT crosses [7].

Our interpretation of the flow cytometry results generated with WT matings was strongly corroborated in crosses with $\Delta HAP2$ strains. In the case of $\Delta HAP2$ × WT crosses (Figure 2D), double-labeled cells were present in the mid-fluorescence gate but were dramatically reduced compared to the same populations in WT × WT crosses (Figure 2C). Furthermore, in $\Delta HAP2$ ×

$\Delta HAP2$ matings (Figure 2E), virtually no double-labeled cells were present in the mid-fluorescence gate and the populations of single-labeled cells (which had not undergone fusion) were overrepresented relative to CFSE^{hi} and CTFR^{hi} populations in WT crosses (Figure 2C).

Based on changes in the median fluorescence intensity (MFI) of the various populations pre- and post-mating, we determined that ~20% of labeled protein in each cell is reciprocally exchanged between WT cells regardless of the tracer or mating type background (Figures 2H and 2I). Interestingly, nearly the identical level of protein transfer was seen in crosses between $\Delta HAP2$ × WT strains (Figure 2I). Thus, despite the reduced rate at which these cells fused (Figure 1R), the overall amount of protein exchanged in the pairs that were capable of fusion was unaffected, suggesting that the initiation of pore formation is the primary defect in $\Delta HAP2$ × WT crosses.

It is also worth noting that, in all instances in which cells of different mating types were mixed, the populations of single-labeled cells that failed to fuse showed an average decline in median fluorescence intensity of ~40% relative to the same populations of cells in cultures that were starved, but not mixed (Figure 2J). This decline in fluorescence was observed in both WT and $\Delta HAP2$ cells and is most likely attributable to “co-stimulation,” a signaling event that occurs when starved cells of different mating types make physical contact and initiate the developmental program that ultimately leads to mating competency. During this transition, alterations in gene expression and protein turnover result in cortical remodeling, which produces a new ventral anterior surface lacking cilia and other subcortical organelles that are required for junction formation between starved cells [12, 14].

To establish a baseline for functional studies with *HAP2* mutant constructs (see below), we performed multiple mass mating experiments with WT, $\Delta HAP2$, and $\Delta HAP2$ rescue strains and determined the mean percentage of cells that fuse in each case (Figure 2G). Consistent with previous fertility data [7], the vast majority of cells in WT × WT crosses fuse, whereas the level is reduced by approximately 75% when *HAP2* is expressed in only one cell of a mating pair. Furthermore, complementation of $\Delta HAP2$ strains with either the genomic or cDNA versions of the *HAP2* gene rescued both the fertility defect [7] and the cell-cell fusion defect in $\Delta HAP2$ × WT crosses as expected (Figure 2G). Overexpression of *HAP2* in WT cells, however, did not rescue fusion in crosses with $\Delta HAP2$ strains (Figures S1A–S1D), reinforcing the idea that the presence of *HAP2* on both sides of the conjugation junction (rather than the total amount of *HAP2* expressed in any given mating pair) is crucial for efficient pore formation in the *Tetrahymena* system.

Predicted Structural Homologies between *HAP2* and Class II Viral Fusogens

As a starting point for the design of mutant constructs, we sought to gain insight into the overall architecture of *T. thermophila* *HAP2* using template-based structural modeling programs, including Phyre2 [15], RaptorX [16], and CPHmodels-3.0. This approach uncovered high (>95%) confidence hits to class II viral fusogens, from which predicted structures could be built. The known structure of a prototypical class II viral fusogen, the dengue virus E glycoprotein (DENV) [17] (PDB ID: 1UZG) is

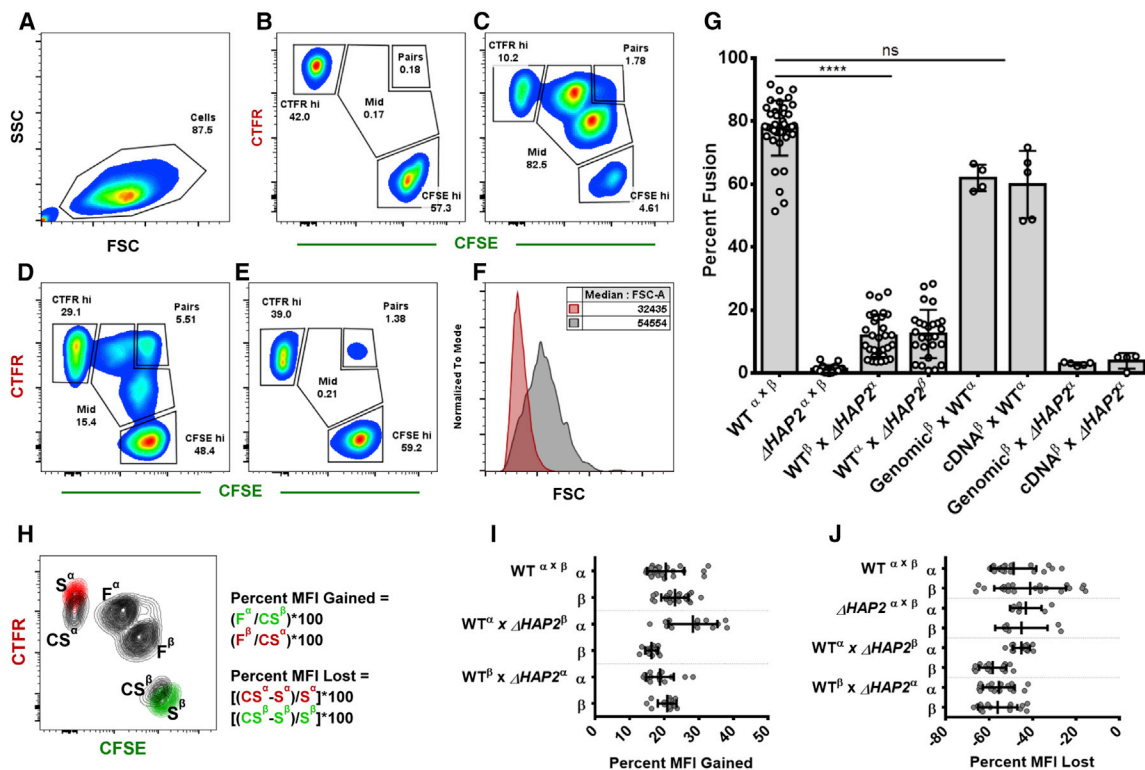


Figure 2. Quantitation of *T. thermophila* Sexual Cell Fusion Events by Flow Cytometry

WT and/or $\Delta HAP2$ cells of different mating types were labeled with either CFSE or CTRF, mixed at a 1:1 ratio, and acquired at different time points after mating and fixation. Superscripts (α and β) denote mating types VII and VI, respectively.

(A) Representative forward scatter (FSC)/side scatter (SSC) plot showing the distribution of cell size versus granularity of a *T. thermophila* mating culture and the gate (circled) chosen for further analysis.

(B) A flow cytometry plot of labeled $WT^\alpha \times WT^\beta$ ($WT^\alpha \times \beta$) cells fixed 15 min after mixing the different mating types.

(C) The same culture as in (B) but instead fixed 16 hr after mixing.

(D) Representative plot of a $WT^\alpha \times \Delta HAP2^\beta$ cross 16 hr after mixing.

(E) Flow cytometry plot of a $\Delta HAP2^\alpha \times \Delta HAP2^\beta$ ($\Delta HAP2^\alpha \times \beta$) cross 16 hr after mixing, showing an absence of events in the mid-fluorescence gate. Numbers adjacent to the outlined areas in (A)–(E) indicate the percent of cells in these gates.

(F) Representative histogram comparing the relative size of individual events (based on forward scatter) in the double-labeled CFSE^{hi}/CTRF^{hi} gate (gray) versus the single-labeled CTRF^{hi} gate (red). Median FSC intensity values for these two populations are shown in the inset.

(G) The cumulative results of independent mass mating experiments, including all biological replicates for different WT, $\Delta HAP2$, and complementation strain crosses (circles represent the percentage of exconjugant cells in the mid-fluorescence gate from individual matings 16 hr after mixing; bar represents mean and error bars \pm SD). “Genomic” or “cDNA” strains are designated according to which *HAP2* gene product was used to complement the $\Delta HAP2$ cell line during their construction. A one-sided Kruskal-Wallis test with a Dunn’s post test found a significant difference (**** $p < 0.0001$) between the $WT^\alpha \times \beta$ cross and $WT^\alpha \times \Delta HAP2$ crosses but no difference (ns, not significant) between the $WT^\alpha \times \beta$ cross and the genomic or cDNA complementation crosses.

(H) Flow cytometry plots of cell populations from mated (dark gray) and unmated (red or green) cultures at the 16 hr time point shown superimposed. Populations of double-labeled cells from the mated cultures are denoted (F), and single-labeled cells that had undergone “co-stimulation” but had not exchanged fluorescent protein are denoted (CS). Note that the populations with the highest fluorescence intensities (MFI) are the single-labeled starved cells (S) from the cultures that had not been mated. The formulas used to measure the “percent MFI gained” (due to transfer of labeled protein from the opposite mating partner) and the “percent MFI lost” (due to co-stimulation) are indicated on the right. The calculations are color coded to show the red or green MFI measurement that was used for each population (S, CS, and F).

(I) Chart showing the mean \pm SD of the percent MFI gained in each mating partner of a given cross, based on the upper formula in (H). The percent MFI gained in F populations was measured with respect to the MFI of the corresponding CS populations, as the co-stimulated partners would theoretically represent the starting fluorescence intensity prior to cellular fusion. Note that no substantial differences were seen in the amount of fluorescent protein exchanged between mating partners in $WT^\alpha \times WT^\beta$ and $\Delta HAP2^\alpha \times WT^\beta$ crosses.

(J) Chart showing the mean \pm SD of the percent MFI lost in each mating type of a given cross based on the lower formula in (H). Regardless of the parental cell lines used, a consistent reduction in the MFI was seen in mated cells that had not undergone fusion (CS) when compared to unmated starved cells (S).

See also Figure S1.

shown in Figure 3A along with the predicted ectodomain structures for *T. thermophila* HAP2 generated by Phyre2 (Figure 3B) and RaptorX (Figure 3C). In the case of Phyre2, the region of homology with DENV covered a 196-amino-acid stretch immedi-

ately upstream of the consensus HAP2/GCS1 domain. This region had only 16% sequence identity but aligned closely to a 166-residue stretch of DENV at the level of predicted secondary structure (Figure 3D). CPHmodels-3.0 identified a similar partial

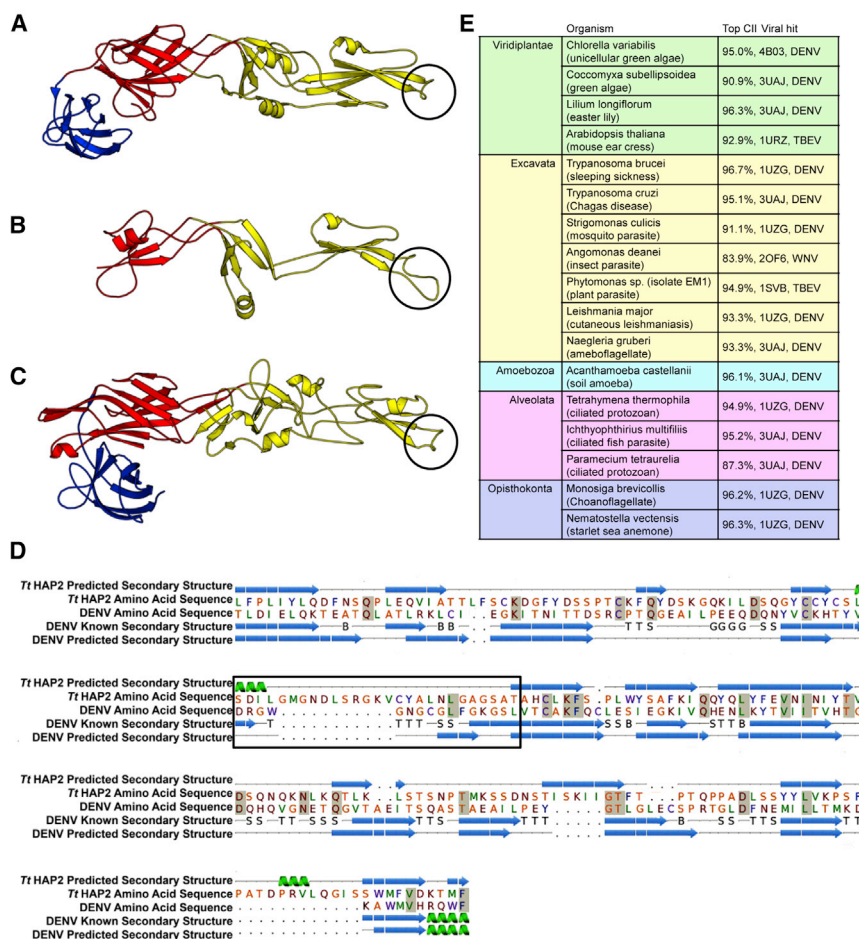


Figure 3. Homology Modeling Predicts a Structural Similarity between HAP2 and Class II Viral Fusogens

The *T. thermophila* HAP2 primary sequence was submitted to template-based structural modeling platforms, Phyre2 and RaptorX. Known and predicted structures shown in (A)–(C) are colored by domain according to the convention used for class II fusion proteins: red, domain I; yellow, domain II (with black circles highlighting the known and predicted fusion loops); and blue, domain III. (A) The known structure of the dengue virus envelope glycoprotein ectodomain (DENV; PDB ID: 1UZG) [17].

(B) The Phyre2-predicted partial structure of the *T. thermophila* HAP2 ectodomain based on the template shown in (A).

(C) The RaptorX-predicted *T. thermophila* HAP2 ectodomain structure based on the Rift Valley fever virus glycoprotein C template (PDB ID: 4HJ1) [18].

(D) Alignment of primary and secondary structural elements in the region of homology between the *T. thermophila* HAP2 ectodomain and dengue virus envelope protein generated by Phyre2. Sequence identities are shaded gray. Secondary structural elements are shown on the top line with α helices indicated by green spirals and β strands by blue arrows. The boxed region is the *T. thermophila* HAP2 sequence aligning to the viral envelope protein's fusion loop.

(E) A table of 17 HAP2 orthologs from other species with the highest confidence hits to class II viral fusogens based on Phyre2 batch processing results (top class II viral hits are listed as % confidence, PDB ID of template envelope protein structure, and viral origin: DENV, dengue virus; TBEV, tick-borne encephalitis virus; WNV, West Nile virus). See also Figure S2 and Table S1.

structural homology to DENV (Figure S2A). The RaptorX homology model predicted a structure for the entire HAP2 ectodomain (Figure 3C) based on a different class II fusion protein template, namely, the Rift Valley fever virus glycoprotein C (PDB ID: 4HJ1) [18]. Together, these structural predictions of HAP2 showed three largely β -sheet-containing domains, analogous to domains I–III of the viral class II fusogens, and included a possible “fusion loop” located at the tip of domain II (circled in Figures 3A–3C; boxed sequence in Figure 3D). The fusion loop in class II viral fusogens inserts into endosomal membranes and is critical for the entry of viral nucleic acid into host cells [19, 20].

A total of 40 HAP2 orthologs [10] were submitted to Phyre2 batch processing [15] to determine the extent to which the predicted structural homology to class II viral fusion proteins is maintained across taxonomic groups. We found that 28 (~70%) had hits to class II viral fusogens (Table S1). A subset of the 17 highest-confidence hits to these viral proteins is shown in Figure 3E.

Mutational Analysis of HAP2 Function

To address the predicted structural similarities between HAP2 and class II viral fusogens, we created cell lines carrying targeted mutations/deletions to specific regions of the *T. thermophila* protein and tested them for functional activity in crosses with WT

cells using flow cytometry. Large deletions to the extracellular region covering either the entire HAP2 domain (Δ 281–329) or the region of alignment with dengue virus E glycoprotein identified by Phyre2 (Δ 93–280) resulted in minimal fusogenic activity (Figures 4A and 4C). The functional relevance of these large deletions was nevertheless unclear, given that both constructs were poorly expressed (Figure S3). Consequently, we began to focus on the region in and around the predicted fusion loop.

In this case, a small 28-amino-acid deletion of the fusion loop itself (Δ 152–179) had a profound effect on fusogenic activity, reducing it to the levels observed in Δ HAP2 \times WT crosses (Figures 4A and 4C). When this deletion was repaired with the native sequence (“HAP2 FL Rescue”; Figures 4A and 4C), the activity was restored to WT levels, but it remained low when a 17-amino-acid sequence comprising the DENV fusion loop was substituted for the predicted HAP2 fusion peptide (“DENV FL Rescue”; Figure 4C). Next, we explored targeted mutations to specific residues in the predicted fusion loop (Figure 4C). The majority of these, including alanine replacements of either LNL171-3 or R164 within the predicted loop itself and replacement of FQY131-3 in a neighboring loop (Figure S2B), had no effect on fusogenic activity (Figure 4C). However, substitutions of serine for the first two cysteine residues (CC147–148SS) in a

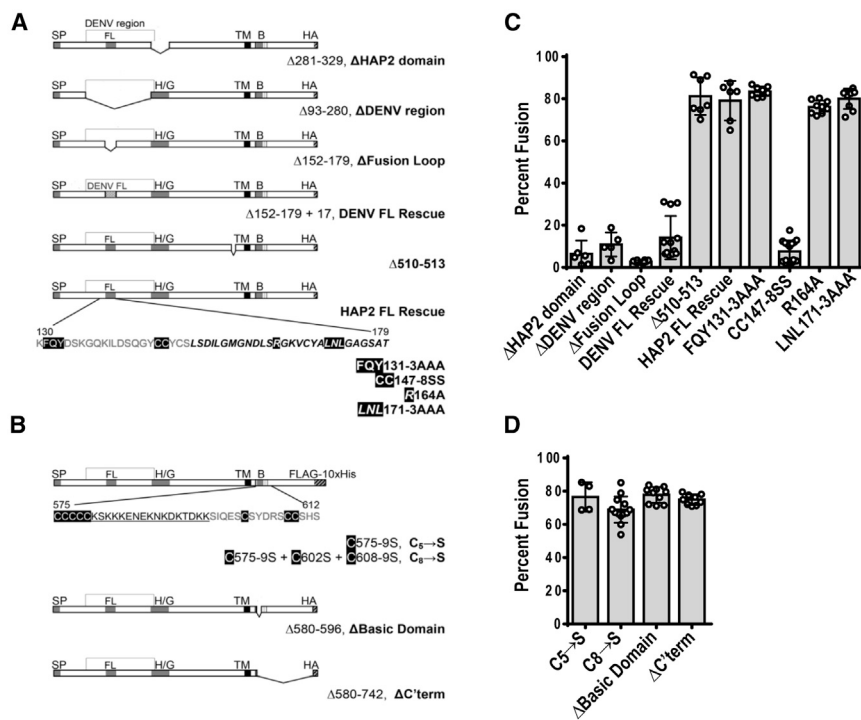


Figure 4. Sequence Elements Important for *T. thermophila* HAP2 Function

Mutant cell lines carrying altered versions of the HAP2 gene were mated with a wild-type (WT) partner and the percentage of cells undergoing fusion determined by flow cytometry. Cell lines that showed levels of fusion equivalent to WT \times β crosses (~80%) were considered to express functional HAP2.

(A) Diagrams of truncations/mutations to the ectodomain. The region in and around the predicted fusion loop is expanded and amino acids targeted for mutations are highlighted in black, whereas those deleted in the fusion loop truncation are shown in bold black, italicized lettering.

(B) Diagrams of truncations/mutations to the cytosolic domain. The region in and around the poly-basic stretch (underlined) is expanded, and the potentially palmitoylated cysteine residues targeted for mutations are highlighted in black. The numbers in (A) and (B) refer to the numerical positions and/or range of truncated amino acids relative to the full-length HAP2 protein sequence. B, poly-basic domain; DENV, Phyre2-predicted dengue virus envelope protein region of homology; FL, fusion loop; FLAG-10xHis, epitope tag; HA, influenza hemagglutinin epitope tag; H/G, HAP2/GCS1 domain; SP, signal peptide; TM, transmembrane domain.

(C and D) Bar charts showing the mean percentage \pm SD of exconjugant cells in the mid-fluorescence gate (cells that had undergone fusion) after mating WT cells with cell lines carrying mutations in the ectodomain (C) or cytosolic domain (D) of *T. thermophila* HAP2 as determined by flow cytometry. Circles represent fusion data from individual matings 16 hr after mixing for the various constructs. A one-sided Kruskal-Wallis with Dunn's post test found no significant differences between the WT \times β cross (Figure 2G) and the HAP2 mutant crosses $\Delta 510-513$, HAP2 FL Rescue, FQY131-3AAA, R164A, LNL171-3AAA, C5→S, Δ Basic Domain, and Δ C'term. A modest yet statistically significant reduction ($p = 0.0011$) in the percentage of fusion was observed for C8→S mutants when compared with the WT \times β cross. Likewise, no significant differences were found between the WT \times Δ HAP2 β cross (shown in Figure 2G) and the HAP2 mutant crosses Δ HAP2 domain, Δ DENV region, Δ Fusion Loop, DENV FL Rescue (C), and CC147-8SS (D). Sample sizes for each cross are listed in the Supplemental Experimental Procedures.

See also Figure S3.

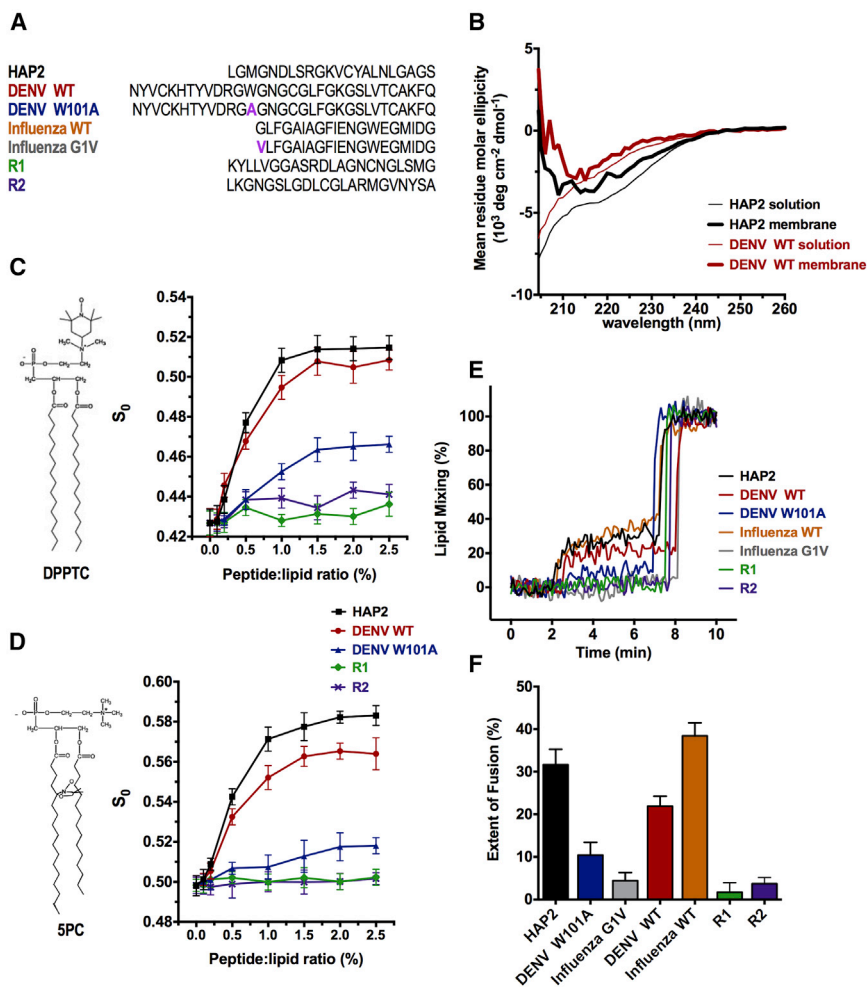
highly conserved cysteine motif that precedes the loop resulted in a dramatic decline in the percentage of cells capable of fusion (Figure 4C). Notably, cysteine residues in the cognate region of class II viral proteins participate in the formation of disulfide bonds that are thought to stabilize the fusion loop [21]. Moreover, in contrast with the large deletions within the ectodomain (above), proteins altered in the region of the fusion loop were expressed and, in almost all cases, correctly localized to the conjugation junction of mating *T. thermophila* (Figure S3).

In addition to mutations to the extracellular region, alterations to the cytosolic domain of *T. thermophila* HAP2 were also constructed (Figure 4B). These included serine substitutions for cysteine residues in some or all predicted palmitoylation sites (C₅ and C₈), deletion of a stretch of highly basic amino acids ($\Delta 580-596$), and deletion of almost the entire cytosolic region (beginning at residue 580). The corresponding mutant proteins were all expressed and correctly localized (Figure S3), and whereas matings with the C₈ substitution showed a slight but statistically significant decrease in fusogenic activity when compared with WT \times WT crosses, the other cytosolic alterations showed no measurable effects (Figure 4D). These results conflict somewhat with data from other systems [8–10], suggesting that the sequence requirements in this region of the protein differ in different organisms.

Biophysical Evidence for Interactions between the HAP2 Fusion Loop and Membranes

The effects of mutations to the HAP2 fusion loop described above, coupled with the known importance of this domain in the activity of class II viral fusogens, clearly suggested that HAP2 and the viral proteins catalyze membrane fusion events through a similar mechanism. To begin to address this question experimentally, we attempted to induce membrane fusion by expressing *Tetrahymena* HAP2 in heterologous systems, namely, mammalian tissue culture cells, and examined the ability of the cells themselves or pseudotyped viruses produced from these cells to undergo fusion (Figures S4A–S4C). Pseudotyped virus particles derived from HAP2-expressing cell lines showed no evidence of infectivity of target cell lines (Figure S4C). Nevertheless, small multi-nucleated syncytia reminiscent of those described by Avinoam and co-workers in studies of the FF family of developmental fusogens [22] were readily observed (Figure S4A). Whereas this result was difficult to quantify, biophysical experiments (see below) clearly demonstrated the ability of the predicted HAP2 fusion loop to interact directly with model membranes.

As revealed by circular dichroism spectroscopy, a synthetic peptide corresponding to the fusion loop of *T. thermophila* HAP2 (Figure 5A) adopts a partially (~30%) β -strand-containing



(F) Bar chart showing the mean and SD (error bars) for normalized percent lipid-mixing data from three independent experiments. All measurements were made at 25°C, and membrane compositions consisted of POPC:POPG:Chol = 5:2:3. See also Figure S4.

structure in the presence of small unilamellar vesicles but is essentially a random coil in solution (Figure 5B). This alteration in secondary structure mimics that observed for a WT DENV fusion peptide under the same conditions and suggests that, as in the case of the viral peptide, the fusion loop of *T. thermophila* HAP2 can bind to membranes.

We then applied electron spin resonance (ESR) spectroscopy to determine whether the predicted HAP2 fusion loop can insert directly into lipid bilayers by measuring changes to the membrane-order parameter, S_0 , of spin-labeled lipids in model membranes in the presence or absence of synthetic peptides. Increased membrane ordering in the presence of viral fusion peptides has been attributed to a membrane dehydration effect in which loosely bound water molecules in the inter-bilayer space move to the bulk water phase. Such peptide-induced changes are thought to be functionally significant as they can lower the energy barrier between closely apposed membranes, allowing fusion to occur [24–26]. Indeed, previous ESR studies with fusion peptides from different class I fusogens (HIV gp41 and influenza hemagglutinin) suggest that this membrane-ordering effect is a

Figure 5. Interaction of the *T. thermophila* HAP2 Fusion Peptide with Model Membranes

(A) Amino acid sequences of synthetic peptides used in biophysical assays (DENV WT, wild-type dengue virus fusion loop; DENV W101A, mutant version of the DENV peptide with reduced fusogenic activity; HAP2, predicted wild-type *T. thermophila* HAP2 fusion loop; influenza WT, wild-type influenza virus fusion peptide; influenza G1V, mutant version of the influenza virus fusion peptide with reduced fusogenic activity; R1, R2, randomized control peptides for the *T. thermophila* HAP2 fusion loop). Amino acid substitutions that reduce fusogenic activity of the mutant viral peptides are indicated in purple letters. All peptides contained a flexible and polar GGGK tag at their C termini (not shown) [23]. (B) Circular dichroism spectra of the DENV and predicted *Tetrahymena* HAP2 fusion loop peptides (2 $\mu\text{g/mL}$; pH 5) in the presence (thick line) or absence (thin line) of small unilamellar vesicles.

(C and D) The head group (C; DPPTC) and acyl chain (D; 5PC) spin-labeled lipids (left) are shown next to their corresponding electron spin resonance (ESR) plots (right). ESR plots depict the order parameter (S_0) of spin-labeled lipids within multilamellar liposome vesicles (y axis) plotted as a function of increasing peptide to lipid ratio (x axis). Data points and error bars represent the mean \pm SD for two (DENV W101A), three (DENV WT and HAP2), or three (R1; R2) independent experiments.

(E) Raw data from a representative lipid mixing experiment showing R18 fluorescence de-quenching over time. Synthetic fusion peptides were added to a mixed population of R18-quenched and unlabeled liposomes at ~ 2 min, followed by Triton X-100 at 7–8 min to establish maximum dequenching values for normalization purposes.

general phenomenon, as well as a critical step for viral membrane fusion [25–27]. Here, we incorporated two different spin-labeled lipids, DPPTC and 5PC, into model membranes to detect peptide-induced changes in membrane structure at both head-group (membrane surface) and acyl chain (hydrophobic bilayer interior) regions, respectively [25]. As shown in Figures 5C and 5D, increasing the peptide:lipid ratio from 0% to 2% resulted in substantial increases in membrane ordering at both the head-group (Figure 5C) and acyl chain regions (Figure 5D) when synthetic peptides corresponding to the predicted HAP2 and DENV WT fusion loops were used. As expected, only a modest increase in membrane ordering was seen with a non-interacting mutant peptide for the dengue virus fusion loop (DENV W101A) [28], whereas control (randomized) peptides corresponding to the HAP2 fusion loop had little to no effect (Figure 5D). In the case of the WT peptides, the roughly S-shaped curves of S_0 as a function of increasing peptide concentrations suggested cooperativity in the membrane-ordering effect, consistent with the requirement for class II proteins to oligomerize for efficient fusion to occur [29]. These data indicate that the respective WT fusion

peptides can insert into membranes and support the idea that the *T. thermophila* HAP2 fusion loop participates in membrane fusion during mating.

To test the fusogenic capacity of the predicted HAP2 fusion loop directly, we conducted lipid-mixing assays with the synthetic peptide from *Tetrahymena* HAP2 and known fusion peptides from both class I and class II viral envelope proteins. In these assays, the lipophilic dye, R18, becomes dequenched and fluoresces upon the merger of labeled and unlabeled large unilamellar vesicles (LUVs). Representative curves of raw data from one of three independent experiments (Figure 5E) show the increase in R18 fluorescence of LUVs between 2 and 7 min following addition of fusion peptide. Figure 5F shows the normalized aggregate results of these experiments. As expected, the non-fusogenic mutant peptides, DENV W101A, and G1V from the influenza hemagglutinin (Figure 5A) promoted only low levels of lipid mixing (10% and 4%, respectively), as did the randomized control peptides for the HAP2 fusion loop ($\leq 4\%$ each). However, like the WT viral fusion peptides, the native *T. thermophila* HAP2 fusion loop peptide promoted high levels of lipid mixing (32% compared to 22% for DENV WT and 38% for influenza WT peptides). Taken together, these data indicate that a synthetic peptide corresponding to the predicted fusion loop of *T. thermophila* HAP2 is capable of interacting directly with membranes, inducing membrane ordering and promoting vesicle fusion.

DISCUSSION

As shown by template-based structural prediction modeling, the ectodomain of *T. thermophila* HAP2 has an overall architecture highly reminiscent of class II viral fusion proteins, forming an extended shape with three, largely β -sheet-containing domains and containing a predicted fusion loop (Figures 3B–3D). A similar topology extends to HAP2 orthologs from a wide array of other species (Figure 3E; Table S1) and has now been validated by X-ray crystallography of the *C. reinhardtii* HAP2 ectodomain [11]. Together with the functional data described here, these studies provide overwhelming evidence that HAP2 is a bona fide membrane fusogen.

Current findings suggest two primary mechanisms by which HAP2 could drive gamete fusion: one used by class II viral fusogens for the invasion of host cells and the other utilized by the structurally related developmental fusogen, EFF-1, to mediate syncytia formation in embryos and larvae of the nematode worm *Caenorhabditis elegans* [30, 31]. In the first case, insertion of a hydrophobic fusion loop into the outer leaflet of endosomal membranes along with structural rearrangements of the protein draw apposed cellular and viral membranes into close proximity, allowing fusion to occur [19]. The developmental fusogen, EFF-1, on the other hand, lacks an obvious fusion peptide and, while adopting the same overall 3D fold as class II viral fusogens, is thought to rely primarily on conformational changes following trans-trimerization of monomers on apposed membranes to drive cell-cell fusion [30]. Consequently, whereas class II viral fusogens are initially present on only one membrane, EFF-1 is required on the surfaces of both apposed membranes in order to induce fusion [22].

With respect to these mechanisms, HAP2 appears sufficient to catalyze membrane fusion when present on only one cell

(i.e., male gametes) in sexually dichotomous species and therefore appears more similar to the viral proteins. In the case of *Tetrahymena*, whereas the rates at which cells of different mating types fuse is reduced when HAP2 is expressed in only one cell of a mating pair, such pairs can still form fusion pores (Figures 2D and 2G). Additionally, like the viral proteins, *T. thermophila* HAP2 contains a functional fusion loop (Figure 4C), and a synthetic peptide corresponding to this region of the protein can mediate lipid mixing by itself (Figures 5E and 5F). Certainly, a hybrid mechanism involving both insertion of a fusion loop (as in the case of the viral proteins) and trans-interactions between proteins on apposed membranes (as has been proposed for EFF-1) remains a possibility for HAP2-mediated fusion in *Tetrahymena*. Future studies will be required to address this and other mechanistic questions related to the specific cellular triggers (e.g., pH, enzymatic processing, and divalent cations) that may regulate these events.

Regardless of the precise mechanism underlying HAP2-mediated membrane fusion, the evolutionary relationship between HAP2 and class II viral fusion proteins is clearly interesting. Whereas it is possible these proteins arose through convergent evolution, the overall topologies and near-identical folding patterns of HAP2 and class II viral fusogens [11] makes this improbable. The alternative hypothesis, namely that they evolved from a common ancestor, is certainly more plausible but leaves open the question of which came first. Recent evidence that similar class II structures are present in phylogenetically distinct virus families has suggested that the coding elements for these proteins arose independently in different viral lineages through the capture of a cellular gene encoding either a developmental fusogen with a class II structure or a bygone viral fusogen piggybacking in the host genome [23, 32]. HAP2, on the other hand, is present within the basal lineages of all major branches of the eukaryotic tree of life and most likely dates to the last common ancestor of all eukaryotes. This would make it the oldest class II fusogen that we know of and thus a strong candidate as the ancestral fusogen from which other class II proteins evolved. At the same time, the existence of viruses pre-dates the evolution of eukaryotic sex [33–36], and it is equally plausible that HAP2 originated with a virus, was exapted for use in gamete cell fusion early in the course of eukaryotic evolution, and was then reacquired by modern viruses. Invasion of eukaryotic genomes by viruses is widespread [32, 37], and there is clear evidence that genes for viral fusogens have taken on new functions in the case of mammalian syncytins, which are of retroviral origin, and promote cell-cell fusion during placentation in diverse species [38, 39].

The strict requirement for cell-cell fusion in sexual reproduction [40] combined with the ancient lineage of HAP2 and its role in fertility in a broad range of taxa [3, 41] argues persuasively for the involvement of this protein in the origin of eukaryotic sex. This argument becomes all the more interesting if HAP2 arose from a virus or related parasitic DNA element, such as a transposon. First, it would suggest that a key step (if not the key step) in fertilization was made possible by a virus. Absent that step, sex and the diversity of life that it spawned (including man) may never have evolved. Second, a role for parasitic DNA in the origin of eukaryotic sex has long been argued. As proposed originally by Donal Hickey, sex may have arisen as

a byproduct of selective pressure on some hypothetical fragment of selfish DNA to spread horizontally from cell to cell, thus favoring its survival [42, 43]. An endogenous viral element or related fragment of parasitic DNA could do this by attaining the capacity to promote cell-cell fusion. Theoretically, this could have occurred through natural selection on a given DNA element (for example, by evolving a coding sequence for a membrane fusogen) or, more simply, through the capture of a gene for a viral fusogen following the infection of some early eukaryotic cell. In either case, the acquisition of such a coding sequence would have served as the starting point for additional evolutionary tinkering to deal with the consequences of fusion, leading eventually to the emergence of karyogamy, meiosis, recombination, and all the modern manifestations of eukaryotic sex.

Whereas the HAP2 gene is deeply rooted in the eukaryotic tree of life, we cannot rule out the possibility that it emerged after the evolution of sexual reproduction, replacing an earlier, perhaps less efficient gamete fusogen. It is also worth noting that important taxonomic lineages, such as fungi and vertebrates, lack HAP2 orthologs. Such sexual species have clearly found an alternative means to accomplish gamete membrane fusion, but whether they use novel proteins or variants of currently known fusion proteins remains to be determined.

SUPPLEMENTAL INFORMATION

Supplemental Information includes Supplemental Experimental Procedures, four figures, and one table and can be found with this article online at <http://dx.doi.org/10.1016/j.cub.2017.01.049>.

AUTHOR CONTRIBUTIONS

J.F.P. designed and performed the majority of the experimental work and wrote the manuscript. A.L.L. designed and performed biophysical assays and helped write the manuscript. J.K.M. designed HAP2 expression experiments in mammalian cells, performed pseudo-typed virus assays, and reviewed the manuscript. D.C.-H. contributed to the experimental design and reviewed the manuscript. J.H.F. designed biophysical studies. T.G.C. designed experiments and wrote the manuscript.

ACKNOWLEDGMENTS

We thank Kelsey Fryer, Daniel Kolbin, Gary Tan, Xueming Dan, Crystal Gergye, Karuna Katariala, Mozammel Hossain, and Catherine Devine for their excellent technical assistance. Dr. William Snell alerted us to a conserved arginine near the HAP2 fusion loop. We thank Drs. Snell, Felix Rey, Juliette Fedry, and Thomas Krey for sharing their data and for bringing the community of researchers studying HAP2 together at the EMBO Conference on Membrane Fusion in Health and Disease (Paris, June 2016). Thanks also to Drs. David Holowka, Maurine Linder, and Gary Whittaker (Cornell University) for their many helpful discussions during the course of the work and to Dr. Garegin Papoian, Hao Wu, and Haiqing Zhao (University of Maryland) for their advice on template-based and ab initio protein modeling. The research reported in this publication was supported by the Office of the Director of the NIH under award number 2P400D010964-12 to T.G.C. and NIH award numbers R01EB003150 and P41GM103521 to J.H.F. and a Graduate Research Fellowship award (DGE-1144153) from the National Science Foundation to J.F.P. Any opinions, findings, and conclusions expressed in this manuscript are those of the authors and do not necessarily reflect the views of the NIH or NSF.

Received: November 18, 2016

Revised: December 31, 2016

Accepted: January 24, 2017

Published: February 23, 2017

REFERENCES

- Johnson, M.A., von Besser, K., Zhou, Q., Smith, E., Aux, G., Patton, D., Levin, J.Z., and Preuss, D. (2004). Arabidopsis hapless mutations define essential gametophytic functions. *Genetics* 168, 971–982.
- Mori, T., Kuroiwa, H., Higashiyama, T., and Kuroiwa, T. (2006). GENERATIVE CELL SPECIFIC 1 is essential for angiosperm fertilization. *Nat. Cell Biol.* 8, 64–71.
- Wong, J.L., and Johnson, M.A. (2010). Is HAP2-GCS1 an ancestral gamete fusogen? *Trends Cell Biol.* 20, 134–141.
- Liu, Y., Tewari, R., Ning, J., Blagborough, A.M., Garbom, S., Pei, J., Grishin, N.V., Steele, R.E., Sinden, R.E., Snell, W.J., and Billker, O. (2008). The conserved plant sterility gene HAP2 functions after attachment of fusogenic membranes in *Chlamydomonas* and *Plasmodium* gametes. *Genes Dev.* 22, 1051–1068.
- von Besser, K., Frank, A.C., Johnson, M.A., and Preuss, D. (2006). Arabidopsis HAP2 (GCS1) is a sperm-specific gene required for pollen tube guidance and fertilization. *Development* 133, 4761–4769.
- Kawai-Toyooka, H., Mori, T., Hamaji, T., Suzuki, M., Olson, B.J.S.C., Uemura, T., Ueda, T., Nakano, A., Toyoda, A., Fujiyama, A., and Nozaki, H. (2014). Sex-specific posttranslational regulation of the gamete fusogen GCS1 in the isogamous volvocine alga *Gonium pectorale*. *Eukaryot. Cell* 13, 648–656.
- Cole, E.S., Cassidy-Hanley, D., Fricke Pinello, J., Zeng, H., Hsueh, M., Kolbin, D., Ozzello, C., Giddings, T., Jr., Winey, M., and Clark, T.G. (2014). Function of the male-gamete-specific fusion protein HAP2 in a seven-sexed ciliate. *Curr. Biol.* 24, 2168–2173.
- Mori, T., Hirai, M., Kuroiwa, T., and Miyagishima, S.Y. (2010). The functional domain of GCS1-based gamete fusion resides in the amino terminus in plant and parasite species. *PLoS ONE* 5, e15957.
- Wong, J.L., Leydon, A.R., and Johnson, M.A. (2010). HAP2(GCS1)-dependent gamete fusion requires a positively charged carboxy-terminal domain. *PLoS Genet.* 6, e1000882.
- Liu, Y., Pei, J., Grishin, N., and Snell, W.J. (2015). The cytoplasmic domain of the gamete membrane fusion protein HAP2 targets the protein to the fusion site in *Chlamydomonas* and regulates the fusion reaction. *Development* 142, 962–971.
- Fedry, J., Liu, Y., Péhau-Arnaudet, G., Pei, J., Li, W., Tortorici, M.A., Traincard, F., Meola, A., Bricogne, G., Grishin, N., et al. (2017). The ancient gamete fusogen HAP2 is a eukaryotic class II fusion protein. *Cell* 168, 904–915.
- Cole, E.S. (2006). The tetrahymena conjugation junction. In *Cell-Cell Channels*, F. Baluska, D. Volkmann, and P.W. Barlow, eds. (Springer), pp. 39–62.
- Parish, C.R. (1999). Fluorescent dyes for lymphocyte migration and proliferation studies. *Immunol. Cell Biol.* 77, 499–508.
- Nasir, A.M., Yang, Q., Chalker, D.L., and Forney, J.D. (2015). SUMOylation is developmentally regulated and required for cell pairing during conjugation in *Tetrahymena thermophila*. *Eukaryot. Cell* 14, 170–181.
- Kelley, L.A., Mezulis, S., Yates, C.M., Wass, M.N., and Sternberg, M.J. (2015). The Phyre2 web portal for protein modeling, prediction and analysis. *Nat. Protoc.* 10, 845–858.
- Källberg, M., Wang, H., Wang, S., Peng, J., Wang, Z., Lu, H., and Xu, J. (2012). Template-based protein structure modeling using the RaptorX web server. *Nat. Protoc.* 7, 1511–1522.
- Modis, Y., Ogata, S., Clements, D., and Harrison, S.C. (2005). Variable surface epitopes in the crystal structure of dengue virus type 3 envelope glycoprotein. *J. Virol.* 79, 1223–1231.
- Dessau, M., and Modis, Y. (2013). Crystal structure of glycoprotein C from Rift Valley fever virus. *Proc. Natl. Acad. Sci. USA* 110, 1696–1701.
- Kielian, M., and Rey, F.A. (2006). Virus membrane-fusion proteins: more than one way to make a hairpin. *Nat. Rev. Microbiol.* 4, 67–76.

20. Zaitseva, E., Yang, S.T., Melikov, K., Pourmal, S., and Chernomordik, L.V. (2010). Dengue virus ensures its fusion in late endosomes using compartment-specific lipids. *PLoS Pathog.* *6*, e1001131.
21. DuBois, R.M., Vaney, M.-C., Tortorici, M.A., Kurdi, R.A., Barba-Spaeth, G., Krey, T., and Rey, F.A. (2013). Functional and evolutionary insight from the crystal structure of rubella virus protein E1. *Nature* *493*, 552–556.
22. Avinoam, O., Fridman, K., Valansi, C., Abutbul, I., Zeev-Ben-Mordehai, T., Maurer, U.E., Sapir, A., Danino, D., Grünewald, K., White, J.M., and Podbilewicz, B. (2011). Conserved eukaryotic fusogens can fuse viral envelopes to cells. *Science* *332*, 589–592.
23. Modis, Y. (2014). Relating structure to evolution in class II viral membrane fusion proteins. *Curr. Opin. Virol.* *5*, 34–41.
24. Chernomordik, L.V., and Kozlov, M.M. (2008). Mechanics of membrane fusion. *Nat. Struct. Mol. Biol.* *15*, 675–683.
25. Ge, M., and Freed, J.H. (2003). Hydration, structure, and molecular interactions in the headgroup region of dioleoylphosphatidylcholine bilayers: an electron spin resonance study. *Biophys. J.* *85*, 4023–4040.
26. Lai, A.L., and Freed, J.H. (2014). HIV gp41 fusion peptide increases membrane ordering in a cholesterol-dependent fashion. *Biophys. J.* *106*, 172–181.
27. Qiao, H., Armstrong, R.T., Melikyan, G.B., Cohen, F.S., and White, J.M. (1999). A specific point mutant at position 1 of the influenza hemagglutinin fusion peptide displays a hemifusion phenotype. *Mol. Biol. Cell* *10*, 2759–2769.
28. Melo, M.N., Sousa, F.J.R., Carneiro, F.A., Castanho, M.A.R.B., Valente, A.P., Almeida, F.C.L., Da Poian, A.T., and Mohana-Borges, R. (2009). Interaction of the Dengue virus fusion peptide with membranes assessed by NMR: The essential role of the envelope protein Trp101 for membrane fusion. *J. Mol. Biol.* *392*, 736–746.
29. Stauffer, F., Melo, M.N., Carneiro, F.A., Sousa, F.J.R., Juliano, M.A., Juliano, L., Mohana-Borges, R., Da Poian, A.T., and Castanho, M.A.R.B. (2008). Interaction between dengue virus fusion peptide and lipid bilayers depends on peptide clustering. *Mol. Membr. Biol.* *25*, 128–138.
30. Pérez-Vargas, J., Krey, T., Valansi, C., Avinoam, O., Haouz, A., Jamin, M., Raveh-Barak, H., Podbilewicz, B., and Rey, F.A. (2014). Structural basis of eukaryotic cell-cell fusion. *Cell* *157*, 407–419.
31. Mohler, W.A., Shemer, G., del Campo, J.J., Valansi, C., Opoku-Serebuoh, E., Scranton, V., Assaf, N., White, J.G., and Podbilewicz, B. (2002). The type I membrane protein EFF-1 is essential for developmental cell fusion. *Dev. Cell* *2*, 355–362.
32. Frame, I.G., Cutfield, J.F., and Poulter, R.T. (2001). New BEL-like LTR-retrotransposons in *Fugu rubripes*, *Caenorhabditis elegans*, and *Drosophila melanogaster*. *Gene* *263*, 219–230.
33. Koonin, E.V. (2009). On the origin of cells and viruses: primordial virus world scenario. *Ann. N Y Acad. Sci.* *1178*, 47–64.
34. Koonin, E.V., Krupovic, M., and Yutin, N. (2015). Evolution of double-stranded DNA viruses of eukaryotes: from bacteriophages to transposons to giant viruses. *Ann. N Y Acad. Sci.* *1341*, 10–24.
35. Cavalier-Smith, T. (2002). Origins of the machinery of recombination and sex. *Heredity (Edinb)* *88*, 125–141.
36. Bell, P.J.L. (2006). Sex and the eukaryotic cell cycle is consistent with a viral ancestry for the eukaryotic nucleus. *J. Theor. Biol.* *243*, 54–63.
37. Katzourakis, A., and Gifford, R.J. (2010). Endogenous viral elements in animal genomes. *PLoS Genet.* *6*, e1001191.
38. Blond, J.-L., Lavillette, D., Cheynet, V., Bouton, O., Oriol, G., Chapel-Fernandes, S., Mandrand, B., Mallet, F., and Cosset, F.-L. (2000). An envelope glycoprotein of the human endogenous retrovirus HERV-W is expressed in the human placenta and fuses cells expressing the type D mammalian retrovirus receptor. *J. Virol.* *74*, 3321–3329.
39. Mi, S., Lee, X., Li, X., Veldman, G.M., Finnerty, H., Racie, L., LaVallie, E., Tang, X.Y., Edouard, P., Howes, S., et al. (2000). Syncytin is a captive retroviral envelope protein involved in human placental morphogenesis. *Nature* *403*, 785–789.
40. Speijer, D., Lukeš, J., and Eliáš, M. (2015). Sex is a ubiquitous, ancient, and inherent attribute of eukaryotic life. *Proc. Natl. Acad. Sci. USA* *112*, 8827–8834.
41. Goodman, C.D., and McFadden, G.I. (2008). Gamete fusion: key protein identified. *Curr. Biol.* *18*, R571–R573.
42. Hickey, D.A. (1982). Selfish DNA: a sexually-transmitted nuclear parasite. *Genetics* *101*, 519–531.
43. Hickey, D.A., and Rose, M.R. (1988). The role of gene transfer in the evolution of eukaryotic sex. In *The Evolution of Sex: An Examination of Current Ideas*, R.E. Michod, and B.R. Levin, eds. (Sinauer Associates), pp. 161–175.